Appl. Phys. B 72, 187–190 (2001) / Digital Object Identifier (DOI) 10.1007/s003400000434

Applied Physics B
Lasers
and Optics

Threshold of oscillation in a ring-loop phase conjugator as a second-order optical phase transition

M. Goul'kov[1], **O. Shinkarenko**[1], **S. Odoulov**[1], **E. Krätzig**[2], **R. Pankrath**[2]

[1] Institute of Physics, National Academy of Sciences, 03650, Kiev-39, Ukraine
[2] Fachbereich Physik, Universität Osnabrück, 49080 Osnabrück, Germany

Received: 10 July 2000/Published online: 20 September 2000 – © Springer-Verlag 2000

Abstract. The threshold behavior is studied for a ring-loop coherent oscillator with a photorefractive strontium barium niobate (SBN) sample. A soft onset of oscillation is revealed and critical slowing down is observed in the temporal development of light-induced scattering below the threshold, thus pointing to a similarity with a second-order phase transition.

PACS: 42.65.Hw; 42.65.Sf; 42.65.P

The onset of oscillation in various photorefractive coherent oscillators may be considered as the transition from a disordered phase (with an arbitrary orientation of scattering gratings of small amplitude) to a phase with a perfect order (only one dominant photorefractive grating with high amplitude) [1–3]. The similarity to phase transitions has been studied in detail for two types of photorefractive coherent oscillators, for a double phase conjugate mirror (DPCM) [2] and for a hexagon-type mirrorless oscillation with two counterpropagating pump waves [3].

It has been shown that the onset of oscillation in a DPCM occurs in a similar way as a second-order phase transition [2], while the hexagon excitation is analogous to a first-order phase transition [3].

From the observation of typical slowing down in the temporal development of the oscillating wave near the threshold of oscillation in a ring-loop phase conjugator, the conclusion was made about the similarity to phase transitions, too [1]. The purpose of the present work is to study the dynamics and steady-state characteristics of the oscillation wave and to confirm a second-order phase transition that might be expected from calculations of the oscillation-wave intensity.

1 Ring-loop coherent oscillator

The geometry of a ring-loop coherent oscillator is depicted in Fig. 1. The pump beam (2) transmitted through a photorefractive sample is reflected back into the sample (4) by the mirrors M_1 and M_2 in such a way that it is overlapping with the beam 2. If the coupling strength of the crystal is sufficiently large

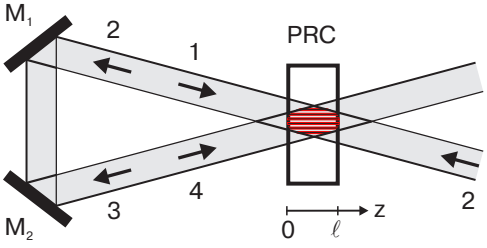

Fig. 1. Schematic representation of a ring-loop coherent oscillator. PRC is a photorefractive crystal, M_1 and M_2 are the cavity mirrors

the oscillation beam appears (waves 3 and 1), which is counterpropagating with respect to the pump beam (waves 2 and 4). The oscillation beam arises because of diffraction of the pump beam from the photorefractive grating developing inside the sample above the oscillation threshold.

The theory of nonlinear mixing of four counterpropagating plane waves with appropriate boundary conditions relates the threshold coupling strength $\gamma\ell_{\rm th}$ necessary to start the oscillation with the cavity mirror reflectivity $R = R_1R_2$ [4, 5]:

$$\gamma\ell_{\rm th} = \frac{R+1}{R-1}\ln\frac{R+1}{2R}. \tag{1}$$

The theory also allows the calculation of the phase conjugate reflectivity (output oscillation intensity normalized to the intensity of the input pump wave) $R_{\rm pc} = I_1(0)/I_2(0)$ as a function of the sample coupling strength $\gamma\ell$ and its threshold value. The dependence of $R_{\rm pc} = R_{\rm pc}(\gamma\ell, \gamma\ell_{\rm th})$ can be found from indirect relations [5]:

$$-\frac{2RT}{T(1-R)+\sqrt{(1-R)^2+4R_{\rm pc}}} = \frac{T(1+R)+\sqrt{(1-R)^2+4R_{\rm pc}}}{T(1-R)+\sqrt{(1-R)^2+4R_{\rm pc}}+2TR_{\rm pc}}, \tag{2}$$

$$T = \tanh\left[\frac{\gamma\ell}{2}\frac{\sqrt{(1-R)^2+4R_{\rm pc}}}{1+R}\right]. \tag{3}$$

Figure 2 represents phase conjugate reflectivity plots (2) and (3) for several different values of R. Two features of the dis-

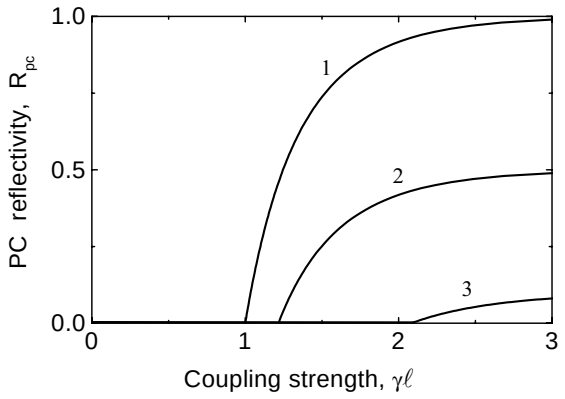

Fig. 2. Calculated coupling-strength dependences of phase conjugate reflectivity for the effective reflectivity of cavity mirrors $M = 1$, 0.5 and 0.1 (*curves* 1, 2 and 3, respectively)

played dependences are of importance from the point of view of the present study: (i) there is no discontinuity in the phase conjugate reflectivity in the vicinity of the threshold and (ii) the phase conjugate reflectivity is a single-valued function of the coupling strength.

This dependence is similar to the dependence of the order parameter versus reciprocal temperature (control parameter) for a ferromagnetic second-order phase transition [6]: there is no ordering at high temperatures (small control parameter $1/T$), while starting from the transition temperature, $1/T_c$, the order parameter increases from the value zero until saturation occurs. It approaches its ultimate value equal to 1 at low temperatures, i.e., at high values of the control parameter $1/T$.

To prove the similarity of the onset of coherent oscillation in a DPCM with a second-order phase transition, the authors of the paper [2] pointed to the formal coincidence of the equation describing the temperature dependence of the normalized magnetization M/M_∞ (order parameter) [6]:

$$M/M_\infty = \tanh\left[MT_c/M_\infty T\right] , \tag{4}$$

where M_∞ is the ultimate magnetization when all spins are aligned, T is the temperature and T_c is the Curie temperature. The equation describing the coupling-strength dependence of the amplitude phase conjugate reflectivity $a = |A_1(0)/A_2(0)| = \sqrt{R_{pc}}$ for a symmetric DPCM reads [7]:

$$a = \tanh\left[a\gamma\ell/\gamma\ell_{th}\right] . \tag{5}$$

At first sight there is no direct correspondence of (1)–(3) to (4). It is possible to show, however, that for a lossless cavity ($R = 1$) the coupling-strength dependence of the phase conjugate reflectivity given by (2) and (3) is exactly the same as (5) (taking into account that the threshold value of the coupling strength for $R = 1$ is $\gamma\ell_{th} = -1$), i.e.,

$$\sqrt{R_{pc}} = \tanh\left[\sqrt{R_{pc}}\gamma\ell/\gamma\ell_{th}\right] . \tag{6}$$

Thus we conclude that the same arguments as presented in [2] apply for the case of a ring-loop cavity, too, i.e., the calculated coupling-strength dependence of $\sqrt{R_{pc}}$ is similar to a standard temperature dependence of the order parameter for a second-order phase transition [6].

In Sect. 2 the results of direct measurements of the oscillation intensity as a function of $\gamma\ell/\gamma\ell_{th}$ are presented that confirm the soft mode of self-excitation, i.e., with an oscillation intensity developing continuously from the noise to a saturation level. Additional arguments in favor of the similarity to a second-order phase transition come from the study of the oscillation dynamics, also described in Sect. 2.

2 Experiments

A ring-loop coherent oscillator with a photorefractive strontium barium niobate (SBN) crystal is studied (Fig. 3). The unexpanded beam of a single-mode multifrequency Ar^+-laser is used as input wave 2, with a total power up to 60 mW and a Gaussian beam waist of 1.5 mm. The coherence length of the pump wave ($\simeq 50$ mm) is much smaller than the loop-cavity length ($\simeq 0.6$ m), to avoid the recording of reflection gratings by counterpropagating waves [8]. The full angle in air between the beams 1 and 4 (2 and 3) is $2\theta_{rec} \simeq 25°$. The sample is slightly tilted to avoid the reflection of wave 4 from the rear face of the sample in the direction of the wave 2 (and reflection of the wave 1 in the direction of the wave 3), i.e., $2\theta_{inc} \simeq 20°$.

With the help of a beam splitter BS a part of the phase conjugate (oscillation) wave 1 is sent to the photodetector PD. The signal from the photodetector is stored and processed with the PC, allowing for reconstruction of the oscillation dynamics. The same computer governs the beam shutter Sh cutting the light beams inside the cavity. When the shutter stops the beams inside the cavity, the incident pump beam 2 erases the photorefractive grating. In such a way the sample becomes ready for the next recording process.

A $Sr_{0.61}Ba_{0.39}Nb_2O_6$:Rh sample (2000 ppm Rh in the melt) grown in the Physics Department of the University of Osnabrück is cut along the crystallographic axes (X, Y, Z) with the dimensions $6 \times 6 \times 7$ mm, respectively. With a loop angle of about 25° the estimated γ is about 20 cm^{-1}, i.e., the coupling strength $\gamma\ell$ is about 12. Therefore one can expect a rather-well-developed coherent os-

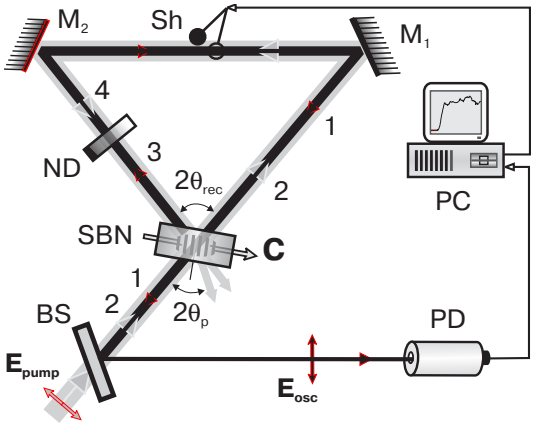

Fig. 3. Experimental set-up. SBN is a strontium barium niobate sample, the *arrow* with C shows the direction of the ferroelectric axis of the sample, M and M_2 are the cavity mirrors, ND is a neutral density filter, Sh is a shutter, BS is a beam splitter, PD is a photodiode, PC is a computer

cillation with $\gamma\ell$ one order of magnitude exceeding the threshold value for the lossless cavity. In fact, the experimental threshold coupling strength is much higher because of the thermal lens developing inside the sample. The sample heated by the incident light wave acts as a converging lens with the focal length comparable to the cavity length; therefore the Gaussian waists of the beams 2 and 4 are not matched, and this affects the threshold value of the coupling strength and the output intensity. Thus the geometry of the ring-loop oscillator was not optimized in our experiment (the estimated normalized coupling strength of the sample was $\gamma\ell/\gamma\ell_{\rm th} \simeq 1.35$ and the largest phase conjugate reflectivity was slightly below 0.02); this was, nevertheless, sufficient for the study of the threshold behavior.

Two techniques are used to change $\gamma\ell/\gamma\ell_{\rm th}$. By putting neutral density filters (ND) inside the loop cavity it is possible to affect the threshold coupling strength $\gamma\ell_{\rm th}$ (see (1) where the effective mirror reflectivity is changing). The coupling strength provided by the sample remains constant in this case. The second technique is to diminish the sample coupling strength keeping the cavity losses (and therefore $\gamma\ell_{\rm th}$) constant. This can be done by rotating the polarization of the input pump wave to a certain angle ϕ with the help of the $\lambda/2$-phase retarder (see, e.g., [2]). Providing the difference in the photoconductivity for the ordinary and the extraordinary waves is negligible the polarization-angle dependence of the coupling strength is as follows:

$$\gamma\ell = \gamma\ell_0 \cos^2\phi, \tag{7}$$

with $\gamma\ell_0$ standing for the initial coupling strength for the extraordinarily polarized pump beam.

Figure 4 shows typical examples of the oscillation dynamics recorded for different cavity losses. The estimated normalized values of the coupling strength are $\gamma\ell/\gamma\ell_{\rm th} \simeq 1.35$, 1.26 and 1.17 for the curves 1, 2 and 3, respectively. Qualitatively, the temporal variations resemble the coupling-strength dependence of the oscillation intensity (see Fig. 2). During a relatively long time the radiation intensity of the cavity modes remains rather small, until the fast nonlinear growth of intensity occurs. A well-pronounced time delay of the rapid growth of oscillation intensity can be considered as a characteristic time of the oscillation onset; it can be measured as a function of the cavity losses or sample coupling strength. The other characteristic to be evaluated from the temporal dependences shown in Fig. 3 is the saturated intensity of the oscillation wave, which is also a function of $\gamma\ell/\gamma\ell_{\rm th}$.

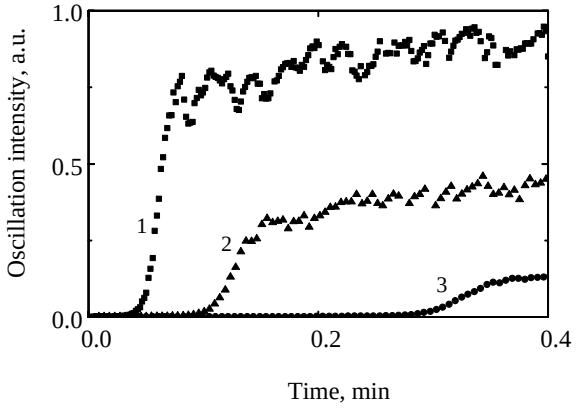

Fig. 4. Dynamics of phase conjugate reflectivity for a coherent oscillator with $\gamma\ell/\gamma\ell_{\rm th} \simeq 1.35$, 1.26 and 1.17 for the *curves* 1, 2 and 3, respectively

2.1 Steady-state characteristics

We first measure the output intensity of the radiation versus polarization angle of the incident pump wave. Figure 5a shows the oscillation intensity as a function of $\varepsilon = (\gamma\ell - \gamma\ell_{\rm th})/\gamma\ell_{\rm th}$ (see, e.g., [9].) Open dots show the intensity of the light-induced scattering below the oscillation threshold, while filled dots represent the oscillation-wave intensity. As the angular aperture of the detector is larger than the angular divergence of the oscillating beam, the detector collects the scattered light not only in the oscillating modes but also in adjacent non-oscillating modes. It means that the intensity of scattered light shown in Fig. 5a is overestimated. In fact, the difference between the saturated intensity of oscillation and the intensity of light scattered in oscillation modes is larger than the value of 2×10^3 which can be deduced from the figure. Thus we observe a very sharp threshold behavior typical for phase transitions.

It should also be emphasized that it is possible to obtain a more than 250-times decrease of oscillation intensity when approaching the threshold with the mechanics available in our experiments for polarization control. One can see that the oscillation intensity is gradually ap-

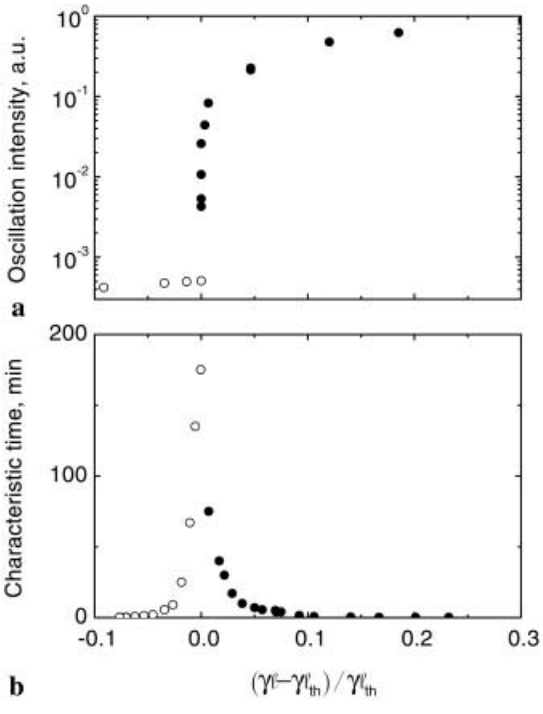

Fig. 5a,b. Steady-state intensity (**a**) and characteristic time (**b**) versus normalized coupling strength ε (see text). The data for light-induced scattering below the threshold are shown by *open dots* and the data for oscillation are shown by *filled dots*

proaching the noise level. We did not observe any difference in the measured dependence for increasing and decreasing $\gamma\ell$.

2.2 Dynamics of oscillation and light-induced scattering

Figure 5b shows the dependence of the characteristic time on the same normalized deviation from the threshold coupling strength as in Fig. 5a, i.e., on ε. In this experiment, however, the cavity losses are controlled by the insertion of neutral density filters with a transparency varying from 0.7 to 0.2. To get more data in the close vicinity of the threshold, filters are used with a difference in the transmittance of 0.01.

Above the threshold, for $\varepsilon > 0$, the delay time of oscillation onset is presented by the filled dots. Below the threshold, for $\varepsilon < 0$, we show by open dots the characteristic time of light-induced scattering, i.e., the time necessary to reach 0.9 of the saturated scattering intensity. Note that we try to measure mainly the scattering into the oscillation modes; a small aperture is put in front of the detector to reduce the contribution from the adjacent non-oscillating modes.

Both processes become obviously slower in the vicinity of the transition. The characteristic time of the light-induced scattering varies from a few seconds (comparable to the dielectric relaxation time) to a few hours. It is important to underline that the dramatic growth of both branches occurs at the same coupling strength equal to the threshold value, $\gamma\ell_{\text{th}}$.

3 Discussion

Both the steady-state characteristics and the dynamics of oscillation point to a similarity of the oscillation onset in the considered geometry and a second-order phase transition: the soft mode of oscillation onset predicted from calculations [4] is confirmed in our experiments with a SBN coherent ring-loop oscillator. No hysteresis behavior is revealed in the coupling-strength dependence of the steady-state oscillation intensity, as one could expect for a second-order phase transition. A considerable slowing down is observed in the development of light-induced scattering near the transition point, analogous to the critical slowing down of fluctuations above an order–disorder phase transition. And, finally, the discontinuity in the characteristic time of light-induced scattering is detected exactly at the same threshold coupling strength where the characteristic delay time of self-oscillation diverges.

Acknowledgements. Financial support of the Deutscheforschungsgemeinschaft (SFB 225) is gratefully acknowledged. We thank M. Segev and M. Mitchell for many stimulating discussions.

References

1. M. Goul'kov, S. Odoulov, R. Troth: Ukr. Phys. J. **36**, 1007 (1991)
2. D. Engin, S. Orlov, M. Segev, G. Valley, A. Yariv: Phys. Rev. Lett. **74**, 1743 (1995)
3. S. Odoulov, M. Goul'kov, O. Shinkarenko: Phys. Rev. Lett. **83**, 3637 (1999)
4. S.-K. Kwong, M. Cronin-Golomb, A. Yariv: IEEE J. Quantum Electron. **QE-22**, 1508 (1986)
5. S. Odoulov, M. Soskin, A. Khizhnyak: *Coherent Oscillators with Degenerate Four-wave Mixing* (Harwood, London, Chur 1998)
6. R. Kubo: *Statistical Mechanics* (North-Holland, Amsterdam 1965)
7. B. Fischer, S. Sternklar, S. Weiss: IEEE J. Quantum Electron. **QE-25**, 550 (1989)
8. M. Cronin-Golomb, J. Paslaski, A. Yariv: Appl. Phys. Lett. **47**, 1131 (1989)
9. S. Ducci, P.L. Ramazza, W. Gonsales-Viñas, F.T. Arecchi: Phys. Rev. Lett. **83**, 5210 (1999)